Supplementary Information (SI) for Environmental Science: Processes & Impacts.

Electronic Supporting Information for Optical properties and photobleaching of wildfire ashes in solution

Frank Leresche,[1,2*] Sarah Fischer,[1,2,3] Shelby Buckley, [1,2,4] and Fernando L. Rosario-Ortiz[1,2*]

[1]Department of Civil, Environmental and Architectural Engineering, University of Colorado at Boulder, Boulder, 80309, USA
[2]Environmental Engineering Program, University of Colorado Boulder, Colorado 80309, USA
[3]Current address, Department of Civil and Environmental Engineering, University of Missouri, Missouri 65201, USA.
[4]Current address, Institute for Biogeochemistry and Pollutant Dynamics, ETH Zurich, Universitaetstrasse 16, 8092 Zurich, Switzerland.

**Correspondence to* Frank Leresche (Frank.Leresche@Colorado.edu)

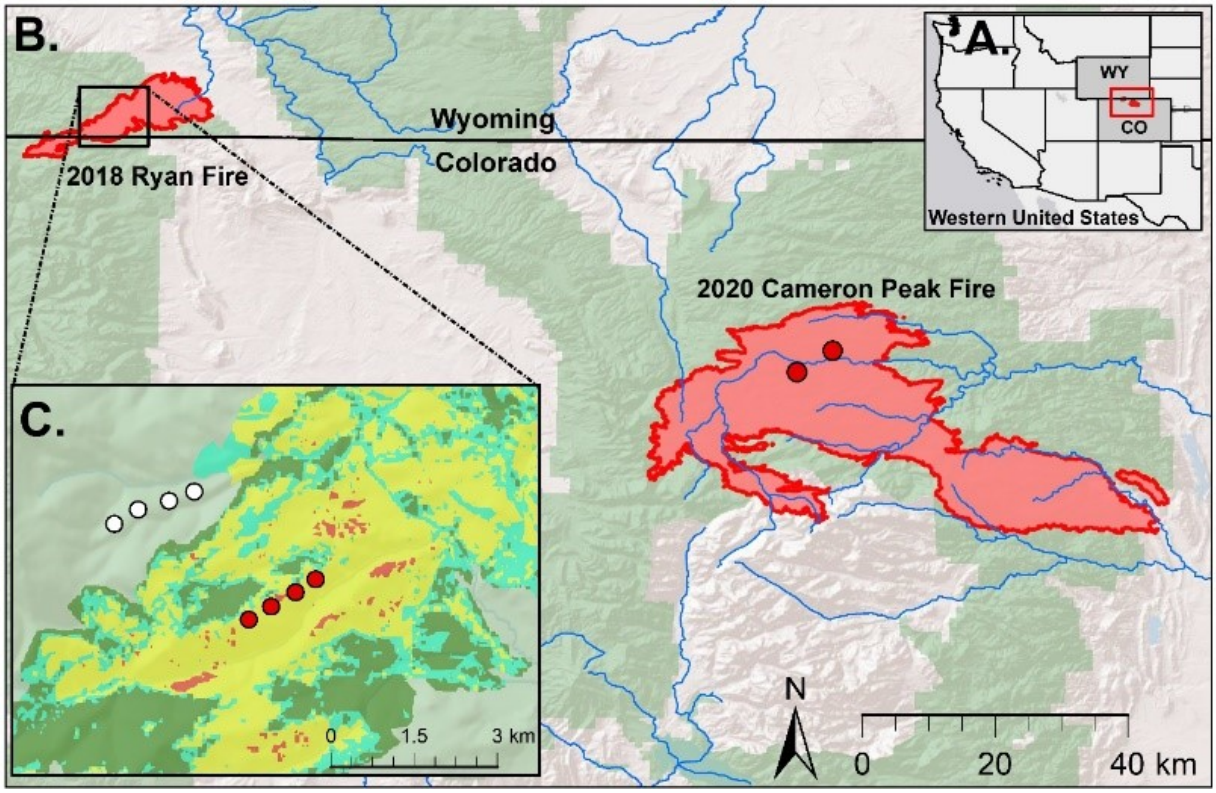

Figure S1. Locations of the Ryan and Cameron Peak Fires where physical ashes (red dots), burned mineral soils (red dots), and unburned mineral soils (white dots) were collected. Map from Fischer et al.[1]

Table S1. Categories and descriptions of soils and ashes leached for photochemical experiments. Number of physical samples tested are listed.

Category	Description
Unburned Soils (n=2)	Ryan Fire burn scar, October 2018, 4 weeks post fire, O horizon from unburned soil outside burn scar,
Burned Mineral Soil (n=6)	Weathered mineral soil (0-10 cm) from old-growth forest in the Ryan Fire burn scar, 1 year post fire
Ash (n=2)	Wildfire ash from the surface of old-growth forest areas, 4 weeks post fire, Ryan Fire Burn Scar
Ash	Grey ash from a high severity patch Black Hollow Creek area of Cameron Peak Fire
Ash	Black ash from a moderate severity patch, Black Hollow, area of Cameron Peak Fire
Ash	Grey ash from a high severity patch, Seven-mile Creek area, area of Cameron Peak Fire

Table S2. Gas chromatography with flame ion detection (GC-FID) and paired nickel catalyst methanizer (NiC) analytical method

Operating Parameters	
Temperatures	
Inlet 100 psi split / splitless	250 ºC
Agilent 40-meter HP-Plot Q Column	100 ºC
NiC Methanizer	375 ºC
Flame Ion Detector	400 ºC
Flow Rates	
Helium (He)	30 mL min^{-1}
Ultra-Grade Air (O_2 and N_2)	400 mL min^{-1}
Hydrogen (H_2)	30 mL min^{-1}
Other Parameters	
Injection Volume	0.5 µL
Total Run Time	11.6 minutes

Compound	**Retention Time (min)**	**Noise (pA)**	**Standard Deviation at Detection (pA)**	**Detection Limit (µM)[2]**	**Quantitation Limit (µM)[3]**
Carbon Dioxide (CO_2)	2.33	0.05	0.127	10.8	20.6

[1] 0.5 µL injection volume and 2.0 mL min^{-1} flow rate.
[2] Detection limit = Blank + 1.645 (Standard Deviation of 25 µM CO_2 standard)
[3] Determined using the standard deviation of the response and the slope method (i.e., signal to noise ratio method of > 10)

Text S1. Singlet oxygen steady-state concentration and quantum yield calculations.

Singlet oxygen ($^1O_2$) steady-state concentration ($[^1O_2]_{ss}$) and quantum yield (Φ_{1O2}) were measured by spiking the solutions with 22.5μM furfuryl alcohol (FFA) as a probe compound in the presence of 0.1M methanol as a hydroxyl radical quencher. Control experiments indicated that FFA direct photolysis is negligible during an experiment (Figure S2). At the used FFA initial concentration, $^1O_2$ main decay pathway in water is physical deactivation with water.[2]

During the course of an experiment, FFA disappearance r_{FFA} (M s^{-1}) is the product of its second-order rate constant towards $^1O_2$ ($k_{FFA,1O2}$=1.00×10^8 M^{-1} s^{-1}),[3] $[^1O_2]_{ss}$ (M) and its concentration (M), but is measured as pseudo-first order rate constant during the experiments (k_{FFA}, unit s^{-1}), equation S1

$$r_{FFA} = k_{FFA,1O2} \times \left[^1O_2\right]_{ss} \times [FFA] = k_{FFA} \times [FFA] \quad \text{(S1)}$$

Rearranging equation S1, $[^1O_2]_{ss}$ can be calculated according to equation S2, using the measured k_{FFA} and the literature value for $k_{FFA,1O2}$:

$$\left[^1O_2\right]_{ss} = \frac{k_{FFA}}{k_{FFA,1O2}} \quad \text{(S2)}$$

Φ_{1O2} that can be considered to be unitless or to have the units of mole $einstein^{-1}$, is by definition the ratio of the singlet oxygen produced ($r_{^1O_2}$, unit M s^{-1}) over the light absorbed (r_{DOM}^{abs}, unit einstein L^{-1} s^{-1}):

$$\phi_{^1O_2} = \frac{r_{^1O_2}}{r_{DOM}^{abs}} \quad \text{(S3)}$$

At steady-state conditions, $r_{^1O_2}$is equal to $^1O_2$ disappearance rate that can be calculated to be the product of $k_{d,1O2,H2O}$ = 2.76×10^5 M^{-1} s^{-1} and $[^1O_2]_{ss}$.[3]

r_{DOM}^{abs} is a function of the photon fluence rate (E_p^0, unit einstein m^{-2} s^{-1}) that was calculated using the *p*-nitroanisole (PNA) pyridine actinometry described in Laszakovits et al.[4] E_p^0 was calculated according to equation S4, where k_{PNA} is the measured phototransformation rate of PNA (unit s^{-1}), Φ_{PNA} is PNA phototransformation quantum yield (Φ_{PNA} = 0.29×[Pyridine]+0.00029, unitless), α and β the lower and upper wavelength integration limits, $f_{p,\lambda}$ the normalized emission spectrum of either the Rayonet photoreactor or of the solar simulator (unitless, see Figure S3), and $\varepsilon_{PNA,\lambda}$ the molar absorption coefficient of PNA at the wavelength λ (unit m^2 mol^{-1}):

$$E_p^0 = \frac{k_{PNA}}{2.303\ \phi_{PNA} \sum_{\alpha}^{\beta} f_{p,\lambda} \varepsilon_{PNA,\lambda}} \quad \text{(S4)}$$

r_{DOM}^{abs} was calculated according to equation S5, where $Abs_\lambda\, l$ is DOM absorbance at the wavelength λ (unit m^{-1}) and l the light path length (unit m):

$$r_{DOM}^{abs} = \frac{1}{1000} \sum_{\alpha}^{\beta} \frac{E_{p,\lambda}^{0}\left(1 - 10^{-Abs_\lambda\, l}\right)}{l} \quad \text{(S5)}$$

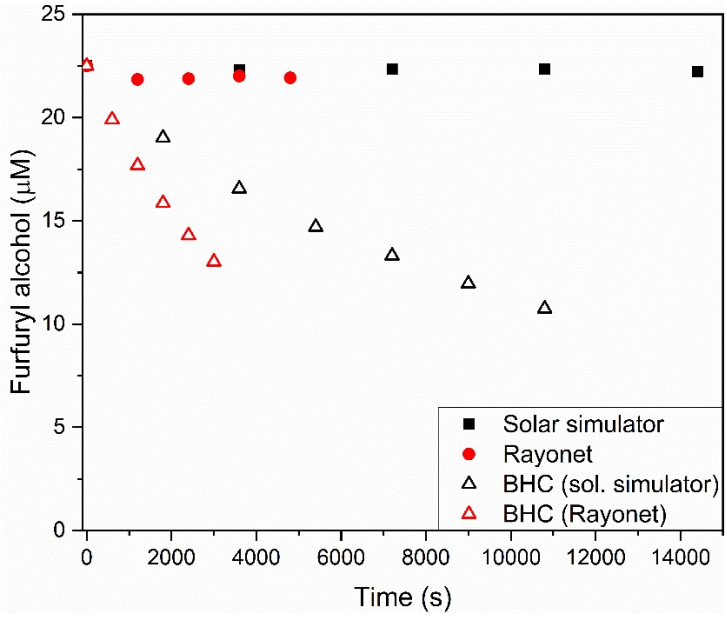

Figure S2. Furfuryl alcohol (FFA) direct photolysis control experiments. Plain black squares and red circles, direct photolysis of FFA in control experiments in ultrapure water under simulated sunlight and in the Rayonet photoreactor. For comparison, FFA concentration in Black Hollow Creek (BHC) samples under simulated sunlight (black hollow triangles) and in the Rayonet photoreactor (red hollow triangles) is also presented.

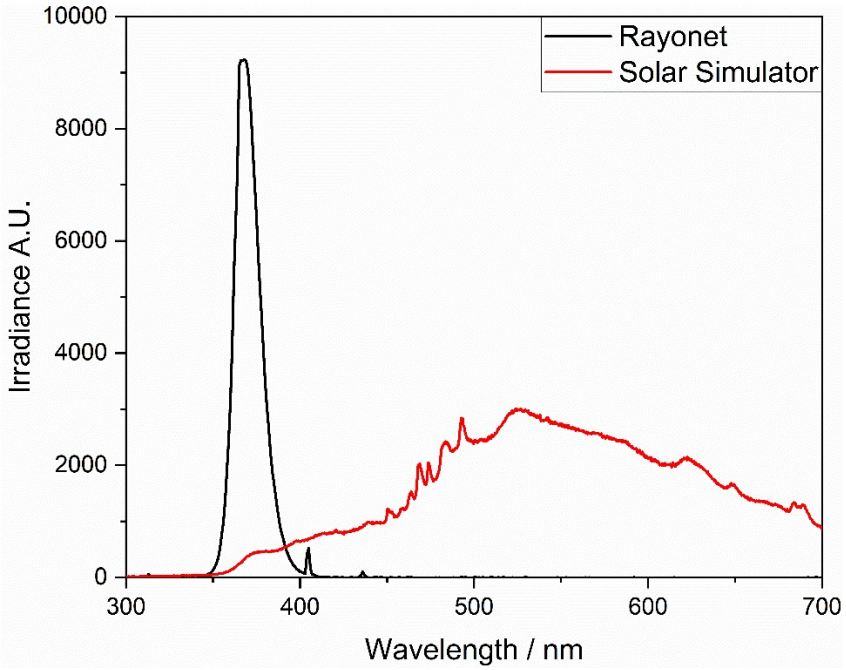

Figure S3. Emission spectra of the Rayonet RPR-3500A lamps and of the Oriel Sol1A solar simulator. Red line, emission spectrum of the solar simulator, Black line, emission spectrum of the Rayonet photoreactor.

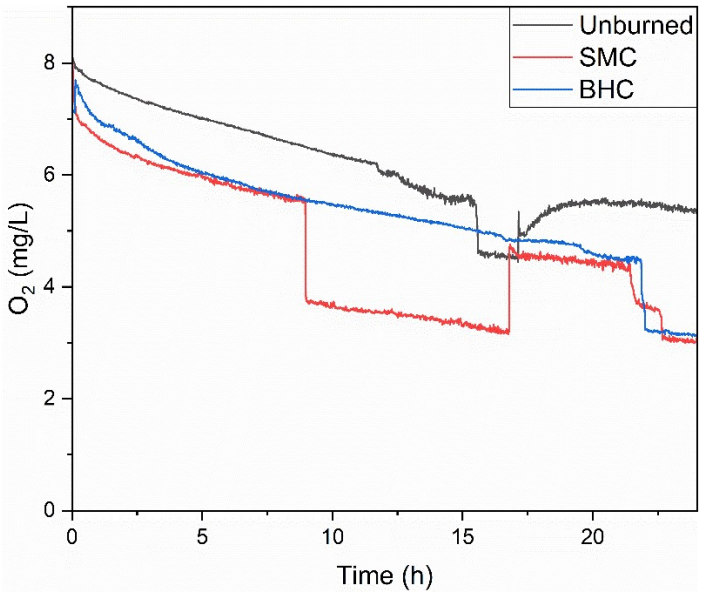

Figure S4. Oxygen evolution during the 24 hours photobleaching experiments. Black, control unburned soil leachate. Red, Seven Mile Creek (SMC) burned soil leachate. Blue, Black Hollow Creek (BHC) burned soil leachate. Note that the sudden drops in [O_2] are believed to be due to issues with the probe measurements.

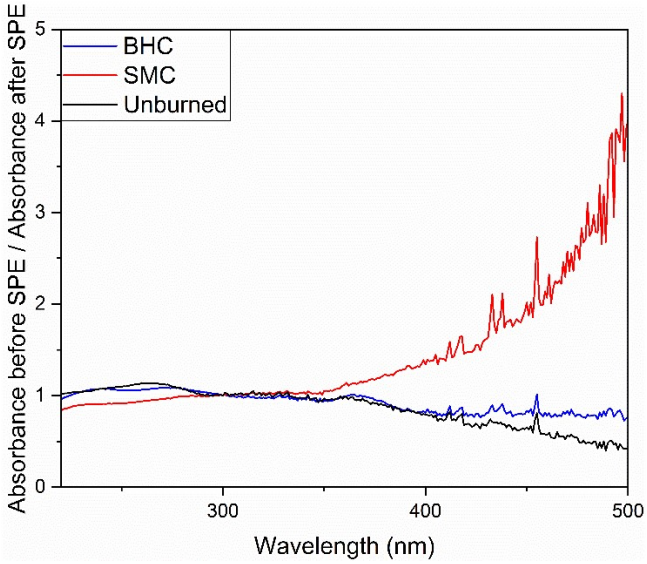

Figure S5. Normalized ration of the absorbance spectra before SPE over after solid phase extraction (SPE), the data was normalized to the wavelength value λ=300nm. Black line, control unburned soil, red line Seven Mile Creek (SMC) wildfire ashes, and blue line Black Hollow wildfire ashes (BHC).

Equation S6. Reaction between ammonium bicarbonate and hydrochloric acid to form CO_2.

$$(NH_4)_2CO_3 + HCl \rightarrow NH_4Cl + CO_2 + H_2O \quad \text{(S6)}$$

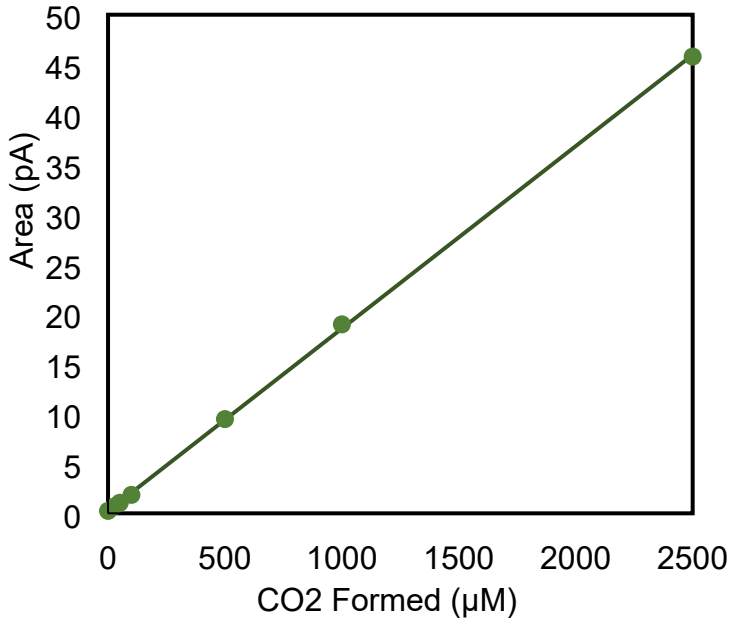

Figure S6. CO_2 calibration curve for gas chromatography and flame ion detection (GC-FID) paired with a nickel catalyst methanizer using acidified ammonium bicarbonate standards ranging from 0 to 2500 µM CO_2.

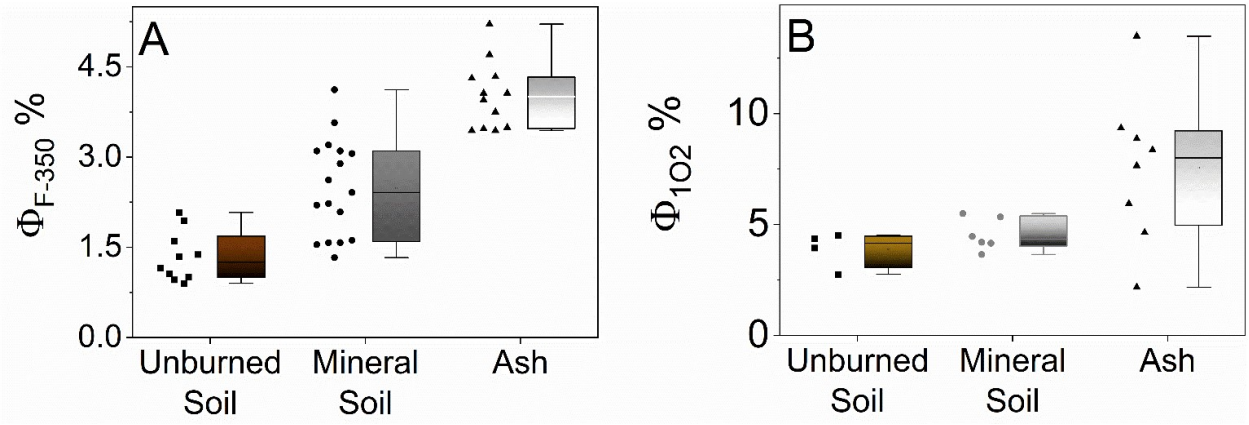

Figure S7. Fluorescence (Φ_F - A) and singlet oxygen quantum yield (Φ_{1O2} - B) for black squares and dark brown box and whisker plot, control unburned soils; black circles and dark grey box plot for mineral soils; and black triangles with a light grey box and whisker plot for surface wildfire ashes. Φ_F is presented for the excitation wavelength λ=350nm (additional Φ_F values for more samples from Fischer et al.[1] are shown in Figure S7A).

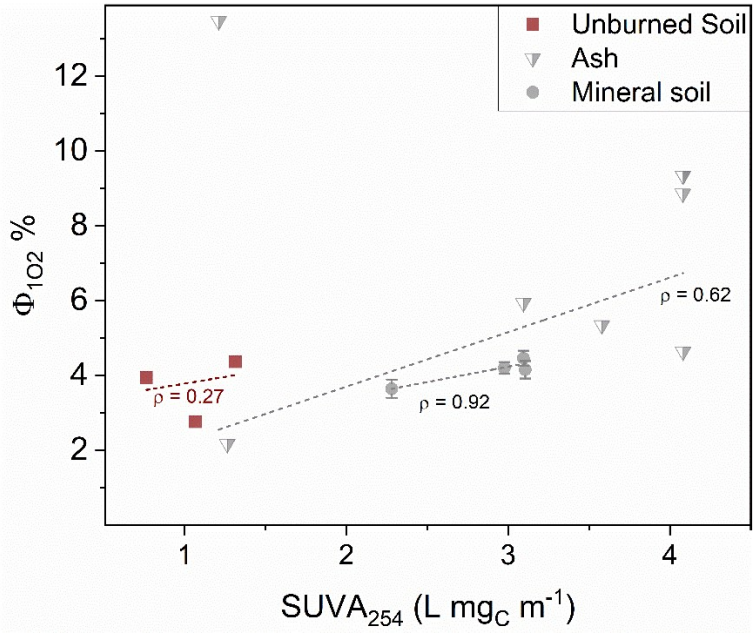

Figure S8. Relationships between $SUVA_{254}$, and singlet oxygen (Φ_{1O2}). Brown squares: control unburned soils, dark grey circles: mineral soils and light grey split triangles: wildfire ashes. $SUVA_{254}$ is the absorbance at 254nm divided by the carbon concentration. The Pearson correlation coefficients (ρ) of the linear regressions are presented for each sample type.

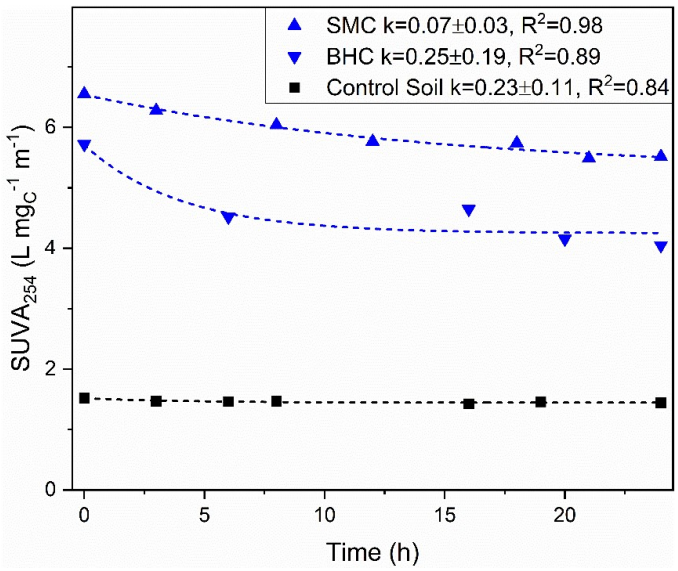

Figure S9. Decrease in specific ultraviolet absorbance at the wavelength λ=254nm ($SUVA_{254}$) of ashes aqueous extracts as a function of irradiation time (simulated sunlight). Dotted lines represent non-linear fitting curves to an exponential function $SUVA = R + S\ e^{-kt}$. Black squares: control unburned soil, upward blue triangles Seven Mile Creek (SMC) wildfire ashes, and downward blue triangles Black Hollow wildfire ashes (BHC).

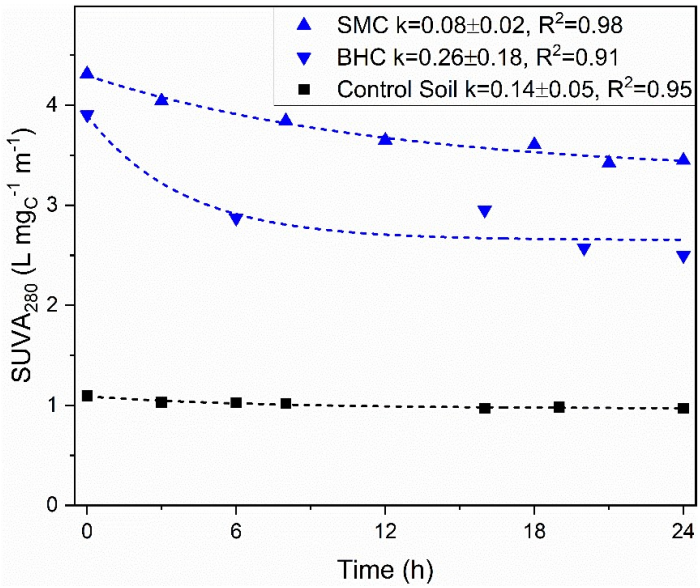

Figure S10. Decrease in specific ultraviolet absorbance at the wavelength λ=280nm ($SUVA_{280}$) of ashes aqueous extracts as a function of irradiation time (simulated sunlight). Dotted lines represent non-linear fitting curves to an exponential function $SUVA = R + S\ e^{-kt}$. Black squares: control unburned soil, upward blue triangles Seven Mile Creek (SMC) wildfire ashes, and downward blue triangles Black Hollow wildfire ashes (BHC).

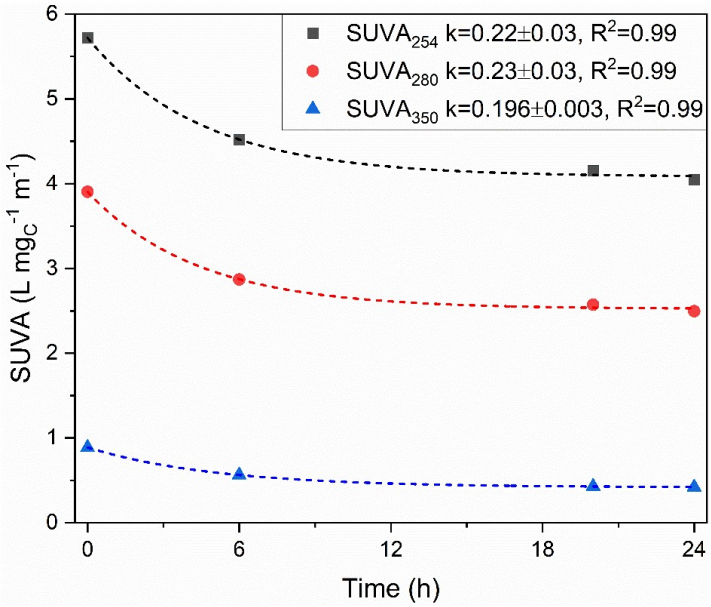

Figure S11. Decrease in specific ultraviolet absorbance (SUVA) of Black Hollow wildfire ashes as a function of irradiation time (simulated sunlight). The data point at time = 16hours was withdraw from this figure. Dotted lines represent non-linear fitting curves to an exponential function SUVA $=R+S\ e^{-kt}$. Black squares: SUVA at the wavelength λ=254nm ($SUVA_{254}$), red circles: SUVA at the wavelength λ=280nm ($SUVA_{280}$), blue triangles: SUVA at the wavelength λ=350nm ($SUVA_{350}$).

Table S3. Non-linear regression parameters from Figure 4 (main text) and Figures S9-S11. Fit to SUVA $=R+S\ e^{-kt}$

	R	S	*k*	R^2	f_s [a]
		Seven Mile Creek wildfire ashes			
$SUVA_{254}$	5.3±0.2	1.3±0.2	0.07±0.03	0.976	19.8%
$SUVA_{280}$	3.31±0.12	0.99±0.11	0.08±0.02	0.982	23.0%
$SUVA_{350}$	0.59±0.02	0.40±0.02	0.15±0.03	0.988	39.7%
		Black Hollow wildfire ashes [b]			
$SUVA_{254}$	4.2±0.2/ 4.08±0.05	1.5±0.3/ 1.63±0.08	0.25±0.19/ 0.22±0.03	0.890/ 0.997	26.2%/ 28.5%
$SUVA_{280}$	2.65±0.15/ 2.52±0.04	1.2±0.3/ 1.38±0.06	0.26±0.18/ 0.23±0.03	0.910/ 0.998	30.7%/ 35.3%
$SUVA_{350}$	0.51±0.11/ 0.4190±0.0018	0.40±0.2/ 0.470±0.003	0.25±0.4/ 0.196±0.003	0.643/ 0.999	45.0%/ 52.9%
		Control Unburned soil			
$SUVA_{254}$	1.444±0.009	0.073±0.016	0.23±0.11	0.841	4.8%
$SUVA_{280}$	0.968±0.012	0.121±0.014	0.14±0.05	0.948	11.0%
$SUVA_{350}$	0.180±0.004	0.088±0.006	0.19±0.03	0.975	32.6%

Note: [a] Calculated as $f_s = S / SUVA_{t=0}$. [b] data including all points/ data excluding the data points at time = 16 hours (Figure S11).

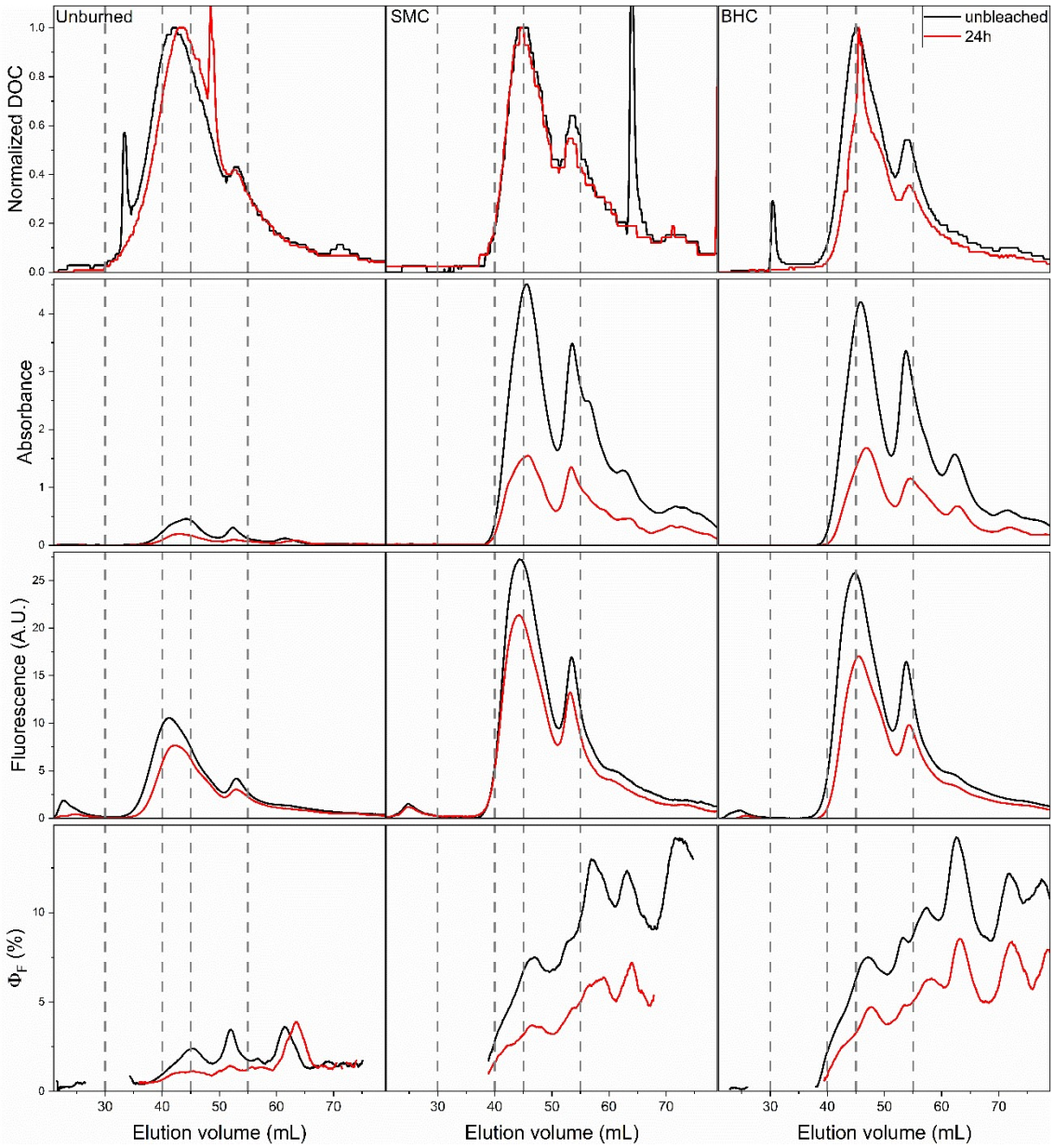

Figure S12. Size-exclusion chromatograms for three ash leachates before (black) and after (red) 24 hours of simulated sunlight irradiation. Left column, control unburned soil leachate, middle column Seven Mile Creek (SMC) ash leachate and right column Black Hollow Creek (BHC) leachate. Dissolved organic carbon (DOC) was normalized to the maximum measured concentration. Absorbance data was smoothed using a ten points fast Fourier filter. Fluorescence quantum yield (Φ_F) was calculated only for data with absorbance value above 0.5 A.U. Notes, apparent molecular weight decreases as elution volume increase, lines at elution volume = 30, 40, 45 and 45mL are presented. They correspond to the different fraction presented in Figure 3. Note, ghost peaks are present in the DOC signal and are believed to be due to an imperfect degassing of the solution and the formation of air bubbles during the SEC measurements. The ghost peaks were withdrawn from the molecular weight fraction calculated in Figure 3.

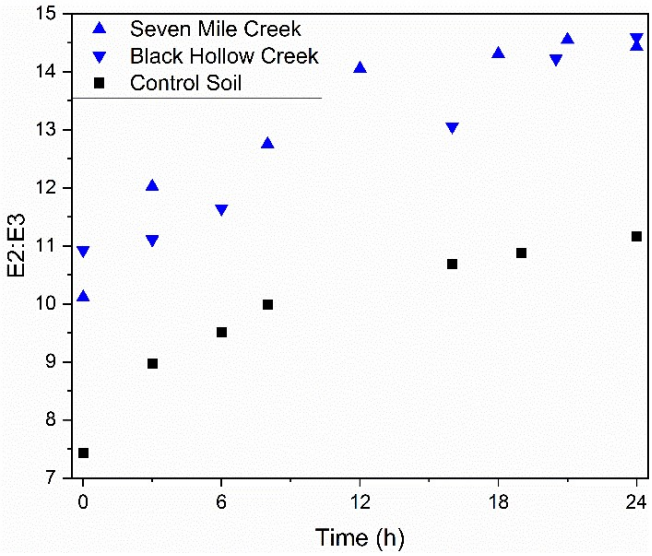

Figure S13. Evolution of E2:E3 parameter (ratio of the absorbance at the wavelength λ=250 over the absorbance at the wavelength λ=365nm) of ashes aqueous extracts as a function of irradiation time (simulated sunlight). Black squares: control unburned soil, upward blue triangles Seven Mile Creek (SMC) wildfire ashes, and downward blue triangles Black Hollow wildfire ashes (BHC).

References for the supporting information

1. Fischer SJ, Fegel TS, Wilkerson PJ, Rivera L, Rhoades CC, Rosario-Ortiz FL. 2023. Fluorescence and absorbance indices for dissolved organic matter from wildfire ash and burned watersheds. ACS ES&T Water. 3(8):2199-2209.
2. Rosario-Ortiz FL, Canonica S. 2016. Probe compounds to assess the photochemical activity of dissolved organic matter. Environ. Sci. Technol. 50(23):12532-12547.
3. Appiani E, Ossola R, Latch DE, Erickson PR, McNeill K. 2017. Aqueous singlet oxygen reaction kinetics of furfuryl alcohol: Effect of temperature, pH, and salt content. Environ. Sci.-Process Impacts. 19(4):507-516.
4. Laszakovits JR, Berg SM, Anderson BG, O'Brien JE, Wammer KH, Sharpless CM. 2017. P-nitroanisole/pyridine and p-nitroacetophenone/pyridine actinometers revisited: Quantum yield in comparison to ferrioxalate. Environ. Sci. Technol. Lett. 4(1):11-14.